Improved retrieval of land ice topography from CryoSat-2 data and its impact for volume change estimation of the Greenland Ice Sheet

Johan Nilsson[1], Alex Gardner[1], Louise Sandberg Sørensen[2] and Rene Forsberg[2]

[1]Jet Propulsion Laboratory, California University of Technology

[2] DTU Space, National Space Institute, Technical University of Denmark

S1 – Surface elevation retrieval

We performed several tests over Greenland to determine the effect of retracking on the accuracy and precision of the measured surface heights from CryoSat-2.

Following the approach of Davis (1997), we have computed the accuracy and precision as a function of the leading edge threshold of the radar waveform. This was done using a standard Leading-edge Threshold retracker (LTH) for the SIN and LRM modes independently. To compute the accuracy and precision, we compared the retracked values of surface elevation to surface elevations measured by the IceBridge ATM (Krabill, 2014b) laser altimeter during a 2013 campaign over Greenland.

For the LRM mode we used data spanning the region 75-81°N and 54-44°W and collected between April and June 2013 to compute height residuals between elevations derived from CryoSat-2 data using a LTH retracker and ATM data. The accuracy was then determined as the mean of the residuals, and the precision as the standard deviation. To remove outliers an iterative 3σ filter was applied to the residuals until a difference of 5% was reached. Only data within 50 m of each ATM location was used for the comparison, providing ~1000 comparison locations. The same procedure was performed for the SIN data over Jakobshavn Isbræ, using the same time period as for the LRM mode. In addition to the LTH results, results from the

Leading edge Maximum Gradient retracker (LMG) were included. This analysis provided roughly ~2500 comparison locations.

The results show that the precision of the LRM mode followed the behavior noted by Davis (1997), with a decrease of precision following an increase in the leading edge retracking threshold (Fig. S1b). However, the most notable finding was the observed inverse relationship between the LRM and SIN mode with respect to precision. For the SIN precision (Fig. S1b), we observed a clear increase in precision as a function of increasing retracking threshold stabilizing above 30-40%.

Studying the accuracy derived from the ATM comparison, there was a clear difference between the apparent penetration depths of the radar signal between the two modes, with SIN elevations tracking closer to the surface. This could be clearly attributed to the difference in the near-surface density structure covered by the two modes. We conclude that application of a low retracking threshold reduces the magnitude of the apparent surface penetration (Figure S1a), and the sensitivity to volume scattering (Figure S1b). Therefore, we recommend the use of thresholds below or around 20% of the maximum power of the leading edge for the LRM mode, previously suggested by Davis (1997) and Helm et al. (2014).

Over the higher relief area defined by the SIN mode mask, in our case Jakobshavn (Figure S1), we found that thresholds below 40% produced either a positive elevation bias (Figure S1a), or low precision, and are therefore not recommended. We found that the LMG retracker used in this study provided superior results compared to the standard LTH retracker. Comparing the optimum result obtained from the LTH algorithm at a threshold of 40%, we found a comparable magnitude of the elevation bias, but also a 32% improvement in precision for the LMG. This provided an overall 27% reduction in the RMS error for the LMG compared to LTH.

S2 – Phase filtering and ambiguity corrections

To determine the effects of the phase filtering and phase ambiguity corrections steps in the SIN-processing on accuracy and precision, a case study was performed over Barnes Ice Cap, Nunavut, Canada. The Barnes Ice Cap was chosen as there was an extensive IceBridge ATM campaign flown there in 2011. The analysis was divided up into four parts. First, both corrections were applied in the processing and compared to ATM elevations within 50 m of each ATM point; second, the phase ambiguity correction was omitted; third, the phase filtering was omitted; and fourth, both corrections were omitted.

The case study was carried out using five months of CryoSat-2 data between February and June 2011. The number of months was selected to maximize the number of comparison samples on this relatively small ice cap. From the statistical analysis (Table S1), we observed that the phase-filtering step accounted for most of the improvement, followed by the phase ambiguity correction.

S3 – Implementation and selection of surface-fit algorithm

For this study a point-by-point (PP) elevation changes estimation procedure was used to derive elevation changes following the approach of Wouters et al. (2015). This solution produced significantly better results than solving for the elevation change rate on a regular grid (RG), as employed by McMillan et al. (2014). The two methods were contrasted by gridding the PP estimated elevation changes onto a regular grid with 1 km resolution and comparing to RG-derived changes of the same resolution. The quality of the solutions was then estimated by comparing to ATM elevation changes over the same time period by means of bilinear interpolation. This produced agreements of 0.09 ± 0.13 m a^{-1} and 0.14 ± 0.21 m a^{-1} for the PP and RG methods respectively, producing a difference in RMSE of 36%. The PP method further exhibited an 80% lower sensitivity to surface slope compared to the RG method.

The higher locality of the solution in the PP method allows for a locally- and globally-higher SNR compared to the RG method. This is due to the fact that the PP method captures the local underlying topography in the solution to a higher degree, making it less sensitive to small-scale surface undulations. In comparison, the grid-based methods solve for the local topography over the entire grid cell area (1 km in this case). Statistically, one might argue that the PP approach has the potential to introduce spatial correlations into the solution; however, studies of the correlation length between the two products compared to ATM elevation change residuals, does not support this argument.

In conclusion, we recommend the use of the point-based solution method (PP) over the grid-based methods (RG), as they provide better agreement with ATM-derived elevation changes, despite the drawback of higher computational cost.

S4 – Validation of surface elevations

We used ATM data spanning four separate years of spring campaigns, largely in the month of April. The estimated surface elevations from the CryoSat-2 mission for both the ESA L2 product and our processing was compared using a search radius of 50 m around each ATM location. The difference between the two measurements was computed as CryoSat-2 minus ATM-formed elevation residuals. The residuals were then edited for outliers using an iterative 3-sigma filter, which stopped once the difference in standard deviation was less than 2%. The results of the surface validation procedure are provided in Tables S2 and S3 and are separated according to their individual modes.

The quality of the four DEMs used in our study (Table S4) was estimated in approximately the same manner as the individual point observations described above, although bilinear interpolation was used instead to estimate the DEM surface elevation at each ATM location. Statistics were then computed for each ATM campaign (Table S4).

S5 – Validation of surface elevation changes

Due to the different time periods used the elevation change errors were multiplied with their individual time spans as elevation change errors should be proportional to the uncertainty in the repeat elevation measurements divided by the time between acquisitions. For the surface-fit method a search radius of 175 m was used which is similar resolution as the ATM elevation changes of 250x250 m (Krabill, 2014a) (product IDHDT4.001). The surface-fit method produces the largest number of validation samples for all time periods. Comparing these results with the crossover method, which used the same search radius for the validation, we found a lower number of validation samples due to the lower spatial coverage produced by this method, further aggravated by the availability of only one time-period for the validation procedure and spatial sampling.

The DEM-based method (Tables S8 and S9) used to produce basin-wide time series exhibited the largest errors, likely due to the smoothing effect for the interpolation and DEM resolution, making it only possible to capture large or medium-wavelength topography (km-scale). This was further confirmed when analyzing the DEM-validation study in Table S4, which shows much larger RMS errors compared to the point analysis. Analyzing Table (S8, S9), we found that the RMSE is significantly larger for the DEM-method, especially for the SIN mode. This can mostly be attributed to the 500 m search radius used to acquire enough samples, which was affected by the local surface slope.

References

Davis, C. H.: A robust threshold retracking algorithm for measuring ice-sheet surface elevation change from satellite radar altimeters, IEEE Trans. Geosci. Remote Sens., 35(4), 974–979, doi:10.1109/36.602540, 1997.

Gray, L., Burgess, D., Copland, L., Demuth, M. N., Dunse, T., Langley, K. and Schuler, T. V.: CryoSat-2 delivers monthly and inter-annual surface elevation change for Arctic ice caps, Cryosphere, 9(5), 1895–1913, doi:10.5194/tc-9-1895-2015, 2015.

Helm, V., Humbert, A. and Miller, H.: Elevation and elevation change of Greenland and Antarctica derived from CryoSat-2, Cryosphere, 8(4), 1539–1559, doi:10.5194/tc-8-1539-2014, 2014.

Khvorostovsky, K. S.: Merging and analysis of elevation time series over Greenland ice sheet from satellite radar altimetry, IEEE Trans. Geosci. Remote Sens., 50(1), 23–36, doi:10.1109/TGRS.2011.2160071, 2012.

Krabill, William B.: IceBridge ATM L4 Surface Elevation Rate of Change [IDHDT4.001], Boulder, Colorado USA, NASA DAAC at the National Snow and Ice Data Center, http://dx.doi.org/10.5067/BCW6CI3TXOCY, 2014a (updated 2015).

Krabill, W. B.: IceBridge ATM L2 Icessn Elevation, Slope, and Roughness, Version 2 [ILATM2], Boulder, Colorado USA, NASA National Snow and Ice Data Center Distributed Active Archive Center, doi: http://dx.doi.org/10.5067/CPRXXK3F39RV, 2014b (updated 2016).

McMillan, M., Shepherd, A., Sundal, A., Briggs, K., Muir, A., Ridout, A., Hogg, A. and Wingham, D.: Increased ice losses from Antarctica detected by CryoSat-2, Geophys. Res. Lett., 41(11), 3899–3905, doi:10.1002/2014GL060111, 2014.

Wouters, B., Martin-Espanol, A., Helm, V., Flament, T., van Wessem, J. M., Ligtenberg, S. R. M., van den Broeke, M. R. and Bamber, J. L.: Dynamic thinning of glaciers on the Southern Antarctic Peninsula, Science, 348(6237), 899–903,

doi:10.1126/science.aaa5727, 2015.

Figures

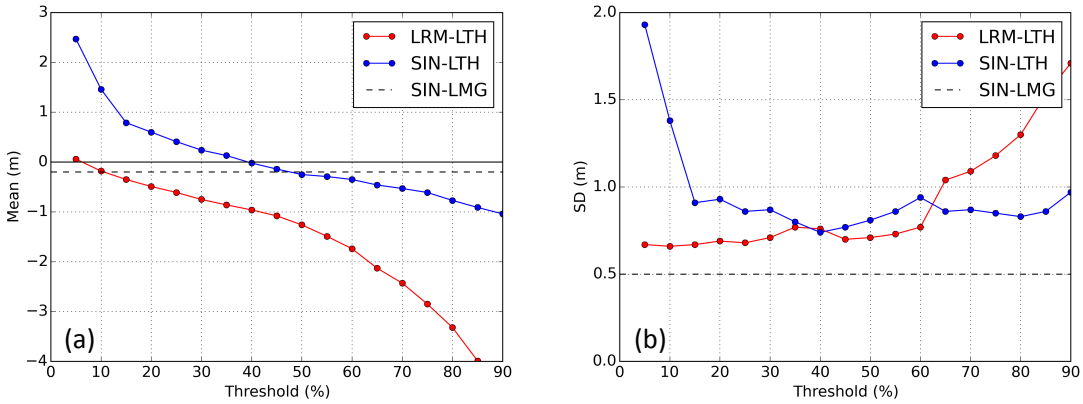

Figure S1: Accuracy (a) and precision (b) of JPL surface elevations, relative to near-coincident ATM elevations, estimated from a Leading-edge Threshold retracker (LTH, dots) over Jakobshavn and NE-Greenland and the Leading-edge Maximum Gradient (LMG retracker, (dashed grey line) for the SIN-mode. The accuracy is defined as the mean-value (Mean) of the CryoSat-2-ATM residuals and the precision as the standard deviation (SD).

Tables

Table S1: Effects on accuracy and precision when omitting SIN-processing steps over Barnes Ice Cap. Four test cases were completed to determine the influence of the different processing steps (phase-filtering and phase ambiguity correction) on the quality of the retrieved observations. Case-1 both the phase-filtering and ambiguity correction applied; Case-2 he ambiguity correction omitted; Case-3 the phase-filtering step omitted; Case-4 both steps have omitted. Statistics were calculated by comparing CryoSat-2 elevations with IceBridge ATM elevations. Here the MEAN is the average of the residuals, SD is the standard deviation, RMSE the Root-Mean-Square-Error, N the number of observations and SE the residual slope error.

Case	Mean (m)	SD (m)	RMSE (m)	N	SE (m/deg)
1	-0.36	0.61	0.71	282	0.35
2	-0.37	0.62	0.72	279	0.37
3	-0.42	0.70	0.82	241	0.32
4	-0.43	0.69	0.82	266	0.46

Table S2: Validation of LRM surface elevations from CryoSat-2 compared to ATM surface elevations. The "Average" row shows the weighted mean-value (using the number of observations) of values. SD is the standard deviation, RMSE the Root-Mean-Square-Error, N the number of observations and SE the residual slope error.

LRM	Mean (m)	SD (m)	RMSE (m)	N	SE (m/deg)
JPL - 2011	-0.18	0.30	0.35	2035	1.16
JPL - 2012	-0.06	0.60	0.60	2443	1.78
JPL - 2013	0.26	0.50	0.57	1054	0.83
JPL - 2014	0.09	0.35	0.36	3025	0.45
Average:	**0.00**	**0.43**	**0.45**	**N/A**	**1.05**
ESA - 2011	-1.36	0.91	1.64	2818	2.58
ESA - 2012	-1.45	1.17	1.87	2874	1.72
ESA - 2013	-0.56	0.71	0.90	1236	1.12
ESA - 2014	-0.70	0.72	1.01	3713	0.84
Average:	**-1.06**	**0.89**	**1.40**	**N/A**	**1.57**

189 *Table S3: Validation of SIN surface elevations from CryoSat-2 compared to ATM surface*
190 *elevations, using CryoSat-2-data from the month of April. The "Average" row shows the*
191 *weighted mean-value (using the number of observations) of values*. SD is the standard
192 deviation, RMSE the Root-Mean-Square-Error, N the number of observations and SE the
193 residual slope error.
194

SIN	Mean (m)	SD (m)	RMSE (m)	N	SE (m/deg)
JPL - 2011	-0.63	0.82	1.03	4475	0.60
JPL - 2012	-0.55	0.57	0.79	4010	0.59
JPL - 2013	-0.37	0.37	0.61	2309	0.47
JPL - 2014	-0.47	0.48	0.76	5504	0.44
Average:	**-0.52**	**0.58**	**0.82**	**N/A**	**0.52**
ESA - 2011	-0.95	1.20	1.53	4355	0.59
ESA - 2012	-1.19	1.31	0.91	4764	0.91
ESA - 2013	-0.76	0.95	1.22	2490	0.38
ESA - 2014	-0.87	0.73	0.96	5203	0.69
Average:	**-0.90**	**1.05**	**1.13**	**N/A**	**0.68**

195

196 *Table S4: Validation of four DEM's using ATM surface elevations from four different campaigns*
197 *over the Greenland Ice Sheet. The "Average" row shows the weighted mean-value (using the*
198 *number of observations) of values.* SD is the standard deviation, RMSE the Root-Mean-Square-
199 Error, N the number of observations and SE the residual slope error.
200

DEM	Mean (m)	SD (m)	RMSE (m)	N	SE (m/deg)
AWI - 2011	-2.03	6.48	6.79	4,216,153	1.26
AWI - 2012	-1.24	5.93	6.06	4,290,351	0.77
AWI - 2013	-0.32	6.74	6.75	2,690,046	2.04
AWI - 2014	-1.41	5.13	5.32	5,314,066	1.54
Average:	**-1.35**	**5.95**	**6.12**	**N/A**	**1.35**
GIMP - 2011	-1.44	7.89	8.02	4,481,612	2.33
GIMP - 2012	-1.35	7.25	7.38	4,427,566	0.35
GIMP - 2013	-0.22	7.40	7.40	2,764,105	0.22
GIMP - 2014	-1.15	6.56	6.66	5,541,920	0.34
Average:	**-1.13**	**7.22**	**7.32**	**N/A**	**0.84**
JPL - 2011	-1.27	6.77	6.89	4,336,066	0.68
JPL - 2012	-1.16	6.14	6.24	4,320,667	2.12
JPL - 2013	0.07	6.81	6.81	2,682,035	1.28
JPL - 2014	-0.79	5.85	5.90	5,443,766	0.41
Average:	**-0.87**	**6.31**	**6.39**	**N/A**	**1.06**
ESA - 2011	-3.48	6.75	7.59	4,321,714	1.14
ESA - 2012	-2.91	5.87	6.55	4,231,174	2.56
ESA - 2013	-2.17	6.80	7.14	2,667,683	2.55
ESA - 2014	-2.57	5.50	6.08	5,356,199	0.82
Average:	**-2.83**	**6.13**	**6.76**	**N/A**	**1.62**

201

Table S5: Validation of SF-SIN surface elevation changes from CryoSat-2 compared to ATM surface elevation changes, using CryoSat-2-data from within a search radius of 175 m of the ATM-locations. The "Average" row shows the weighted mean-value (using the number of observations) of values SD is the standard deviation, RMSE the Root-Mean-Square-Error, N the number of observations and SE the residual slope error

SF - SIN	Mean (m)	SD (m)	RMSE (m)	N	SE (m/deg)
JPL – 2011-13	0.36	0.68	0.78	20,051	0.10
JPL – 2011-14	0.33	0.57	0.66	102,613	0.42
JPL – 2012-14	0.26	0.58	0.64	94,630	0.82
Average:	**0.30**	**0.58**	**0.66**	**N/A**	**0.52**
ESA – 2011-13	0.48	1.18	1.26	22,844	0.10
ESA – 2011-14	0.33	0.99	1.05	112,091	0.54
ESA – 2012-14	0.32	1.10	1.14	101,042	0.30
Average:	**0.34**	**1.06**	**1.11**	**N/A**	**0.39**

Table S6: Validation of SF-LRM surface elevation changes from CryoSat-2 compared to ATM surface elevation changes, using CryoSat-2-data The "Average" row shows the weighted mean-value (using the number of observations) of values. SD is the standard deviation, RMSE the Root-Mean-Square-Error, N the number of observations and SE the residual slope error

SF - LRM	Mean (m)	SD (m)	RMSE (m)	N	SE (m/deg)
JPL – 2011-13	0.32	0.56	0.64	6,639	0.24
JPL – 2011-14	0.18	0.69	0.69	14,643	0.72
JPL – 2012-14	-0.02	0.70	0.70	18,950	0.20
Average:	**0.11**	**0.67**	**0.69**	**N/A**	**0.39**
ESA – 2011-13	0.66	1.56	1.70	8,679	1.84
ESA – 2011-14	0.54	1.50	1.59	18,142	1.77
ESA – 2012-14	-0.20	1.50	1.50	19,846	0.86
Average:	**0.25**	**1.51**	**1.57**	**N/A**	**1.40**

227 *Table S7: Validation of XO crossover surface elevation changes from CryoSat-2 (2011-2014)*
228 *compared to ATM surface elevation changes.* SD is the standard deviation, RMSE the Root-
229 Mean-Square-Error, N the number of observations and SE the residual slope error.
230

XO - LRM	Mean (m)	SD (m)	RMSE (m)	N	SE (m/deg)
JPL	0.24	0.72	0.78	683	1.23
ESA	0.60	1.02	1.20	557	5.01
XO - SIN					
JPL	-0.06	1.26	1.26	12,075	0.60
ESA	-0.21	1.44	1.44	10,477	0.81

231

232

Table S8: Validation of DM-SIN surface elevation changes from CryoSat-2 compared to ATM surface elevation changes. The "Average" row shows the weighted mean-value (using the number of observations) of values. SD is the standard deviation, RMSE the Root-Mean-Square-Error, N the number of observations and SE the residual slope error.

DM - SIN	Mean (m)	SD (m)	RMSE (m)	N	SE (m/deg)
JPL – 2011-13	0.76	5.18	5.24	2,149	7.30
JPL – 2011-14	0.42	3.63	3.66	4,513	7.41
JPL – 2012-14	-0.10	3.12	3.12	5,002	1.76
Average:	**0.26**	**3.59**	**3.72**	**N/A**	**4.97**
ESA – 2011-13	1.32	7.56	7.66	2,197	2.04
ESA – 2011-14	0.09	5.28	5.28	4,925	2.91
ESA – 2012-14	0.10	3.74	3.74	5,403	3.64
Average:	**0.31**	**5.01**	**5.03**	**N/A**	**3.07**

Table S9: Validation of DM-LRM surface elevation changes from CryoSat-2 compared to ATM surface elevation changes. The "Average" row shows the weighted mean-value (using the number of observations) of values. SD is the standard deviation, RMSE the Root-Mean-Square-Error, N the number of observations and SE the residual slope error.

DM - LRM	Mean (m)	SD (m)	RMSE (m)	N	SE (m/deg)
JPL – 2011-13	-0.30	5.02	5.04	1,428	4.04
JPL – 2011-14	0.12	1.74	1.74	3,554	0.24
JPL – 2012-14	0.36	1.38	1.42	6,888	0.22
Average:	**0.21**	**1.92**	**1.95**	**N/A**	**0.68**
ESA – 2011-13	-2.48	10.00	10.30	1,153	15.66
ESA – 2011-14	0.15	1.50	1.53	3,300	2.76
ESA – 2012-14	0.80	1.54	1.74	6,780	1.58
Average:	**0.27**	**2.40**	**2.56**	**N/A**	**3.37**